Red-emitting $Al_2O_3:Eu^{3+}$ Phosphor Powders Featuring Sheet Morphology for the Application of Fingerprint Revealing

María Fernanda IBARRA [1], David Alejandro CHÁVEZ CAMPOS [2], Alejandro NÚÑEZ VILCHIS [1], María Guadalupe GODINA CUBILLO [2], José Luis FRAGA ALMANZA [2], Jorge OLIVA UC [3], Carlos Eduardo RODRIGUEZ GARCIA [2] *

[1] *Facultad de Química, Universidad Autónoma de Querétaro, Cerro de las Campanas S/N-Edificio 5, Centro Universitario, 76017 Santiago de Querétaro, Qro. México*
[2] *Facultad de Ciencias Físico Matemáticas, Universidad Autónoma de Coahuila, Edif. A, Saltillo, S/N, 25280 Saltillo Coahuila, México*
[3] *Centro de Física Aplicada y Tecnología Avanzada (CFATA), Universidad Nacional Autónoma de México, Blvd. Juriquilla No. 3001, campus Juriquilla 76230 Santiago de Querétaro, México*

http://doi.org/10.5755/j02.ms.37726

Received 25 June 2024; accepted 28 November 2024

In this work, $Al_2O_3:xEu^{3+}$ red phosphor powders were produced by the combustion synthesis technique with different x molar percentage concentrations of doping of x = 1.5, 3.0, 5.0, and 7.0 mol% of Eu. X-ray diffraction analysis demonstrated that the powders present the Al_2O_3 crystalline phase. Scanning electron microscopy discovered a sheet-like morphology in the $Al_2O_3:xEu^{3+}$ phosphor samples. The sheet particle sizes are in the range of 40 – 280 μm and with an average thickness of 4.8 μm. Photoluminescence measurements of the samples under 254 nm excitation, showed two main red emission peaks at 615 nm and 700 nm attributed to Eu^{3+} luminescent transitions, $^5D_0$-$^7F_2$, $^5D_0$-$^7F_4$, respectively. The $Al_2O_3:xEu^{3+}$ red phosphors were applied for fingerprint revealing application on different surfaces and in crime scenes. The fingerprints were successfully revealed on steel, plastic, and ceramic surfaces, and photographs of the revealed fingerprints were taken. Several fingerprint features, such as short ridges, eyes, bifurcations, cores, and right loop elements, were clearly detected and sharply defined in the photographs. Therefore, the $Al_2O_3:xEu^{3+}$ red phosphors show potential as an effective material for fingerprint detection in forensic science applications.
Keywords: luminescence, fingerprints, aluminum oxide, europium.

1. INTRODUCTION

Rare earth elements (REEs) have been employed as dopants in crystalline hosts to achieve luminescence characterized by superior lifetime, high efficiency, reliability, and notable energy conservation. Among REEs, Eu^{3+} stands out as one of the most effective dopants for generating red emission in host materials, exhibiting a prominent emission peak at approximately 616 nm, attributed to the f-f transition $^5D_0$-$^7F_2$ [1].

In recent years, luminescent RE-doped oxide phosphors have garnered significant attention due to their high brightness and diverse color emissions. The advantages of RE-doped oxide phosphors include their thermal and chemical stability compared to sulfide-based phosphors [2]. Among oxide materials, aluminum oxide (Al_2O_3), commonly known as alumina, serves various industrial purposes such as catalysts, abrasives, and insulators, owing to its favorable thermal and chemical properties [3]. When doped with Eu^{3+}, Al_2O_3:(referred to as $Al_2O_3:Eu^{3+}$) exhibits strong red emission attributable to the 4f-4f Eu^{3+} forbidden transitions [4]. It has demonstrated excellent hosting properties due to its low phonon energy, indicating infrequent atomic vibrational movements upon excitation by low-UV light, thereby enabling visible light emission without absorption at visible light wavelengths [5].

The crystalline powder $Al_2O_3:Eu^{3+}$ has been reported in the literature and synthesized using various soft chemistry methodologies including the microwave solvothermal method, sol-gel technique, hydrothermal method, metal-organic decomposition (MOD), or combustion synthesis [6]. While the sol-gel technique is widely used, it presents significant drawbacks such as environmental pollution and high cost [7]. Hence, in this study, we opted for the combustion synthesis method using urea as the organic fuel, known for its efficacy in aluminum compound synthesis [8].

The $Al_2O_3:Eu^{3+}$ phosphors synthesized in this research allowed for the characterization of their red emission across different doping concentrations, identification of the crystalline phase adopted, and elucidation of their sheet-like morphology and associated luminescent capabilities. Furthermore, the Eu-doped Al_2O_3 phosphors were evaluated for their utility in developing fingerprint samples and their interaction with materials commonly encountered at crime scenes, such as metallic knives, ceramic mugs, and credit cards. These surfaces, particularly fluorescent ones, pose challenges in forensic science due to the difficulty of revealing fingerprints.

* Corresponding author. Tel.: +52-844-3483655.
E-mail: *crodriguezgarcia@uadec.edu.mx* (C.E. Rodriguez Garcia)

2. EXPERIMENTAL DETAILS

2.1. Synthesis of $Al_2O_3:Eu^{3+}$ phosphors

Europium nitrate [$Eu(NO_3)_3$, 99.9 %], aluminum nitrate [$Al(NO_3)_3$ $9H_2O$, 98.0 %], and urea [$CO(NH_2)_2$, 99.0 %] were acquired from Sigma-Aldrich. The $Al_2O_3:Eu^{3+}$ phosphors were synthesized through a combustion method, varying the Eu dopant concentrations from 1.5 to 7.0 mol% in the $Al_2O_3:xEu^{3+}$. In a typical synthesis, stoichiometric amounts of the nitrates were mixed in 20 mL of distilled water until they dissolved in a borosilicate glass beaker. The mixture was then placed in a pre-heated muffle furnace at 500 °C for 15 minutes, initiating the combustion process. This resulted in the escape of gases during the chemical reaction, producing a white, voluminous, foamy, and highly porous ash through self-ignition with a bright flame. Subsequently, this ash was allowed to cool and then ground into a fine powder using a mortar and pestle. The synthesized powder underwent heat treatment at 1000 °C for 1 hour in air.

The surface morphology of the $Al_2O_3:xEu^{3+}$ samples was visualized using scanning electron microscopy (SEM) (Jeol JSM-7410F operated at 200 kV), and the X-ray diffraction patterns (XRD) were recorded using a Bruker D8 Avance Eco instrument with Cu-Kα radiation (λ = 1.5406 Å). Photoluminescence (PL) spectra were obtained using a Shimadzu RF 6000 Spectrofluorometer, with an excitation wavelength of 254 nm.

2.2. Fingerprint detection procedure

The $Al_2O_3:xEu^{3+}$ samples were pulverized using a mortar and pestle and then sprinkled onto fingerprints deposited on four different common surfaces found at crime scenes: a knife, a cup, a credit card, and eyeglasses. The fingerprint detection procedure involved weighing 0.2 mg of $Al_2O_3:Eu^{3+}$ phosphorescent powder, followed by the application of the fingerprint by a human donor using a camel-hair brush. Photographs were acquired using a 12-megapixel camera after one minute of surface excitation with a 365 nm UV lamp.

2.3. X-ray diffraction analysis

The characterization of $Al_2O_3:xEu^{3+}$ samples revealed the successful observation of the desired phase of Al_2O_3 according to the data from PDF #37-1462. However, in the sample containing a molar percentage of x = 7.0 % of Europium, spurious phases of corundum were also detected (PDF #46-1212) [9], these peaks were labeled with the symbol "*" in Fig. 1 a.

2.4. Scanning electron microscopy analysis

SEM images were taken of Al_2O_3 doped with Eu^{3+} at four different concentrations: 1.5 %, 3.0 %, 5.0 %, and 7.0 mol%, with a magnification of 1000×. All samples exhibited a consistent structure, characterized by sheet- or flake-like morphologies, porosity, and waviness, as shown in Fig. 1 b. Using ImageJ software, we measured the size of the sheet, their pores, and their thickness to determine the average, maximum, and minimum values. The sample with the most promising luminescent properties (3.0 %) displayed the largest sheet, with an average size of 177.88 μm. The largest sheet measured 278.58 μm, while the smallest was 98.85 μm. The pore density within the sheet was low, with only 15 data points collected, resulting in an average pore size of 3.67 μm, ranging from 1.67 μm to 6.07 μm. Similarly, this sample exhibited the thinnest sheet, with an average thickness of 2.87 μm. The structure observed in this study has been previously reported, as it develops after the foam formation during the initial firing in the muffle furnace, followed by water evaporation during the heat treatment process [10]. Administering a higher concentration of Eu^{3+} ions can not only fail to enhance the luminescent properties of Al_2O_3 but also lead to the formation of smaller, more porous, and thicker crystals.

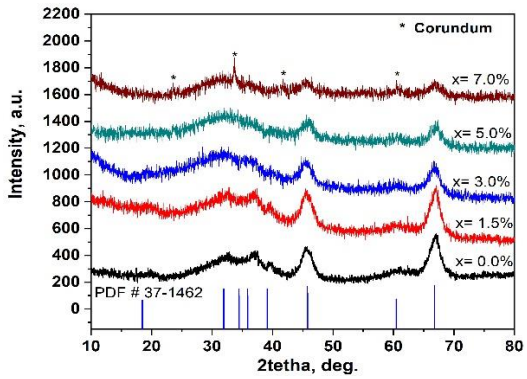

a

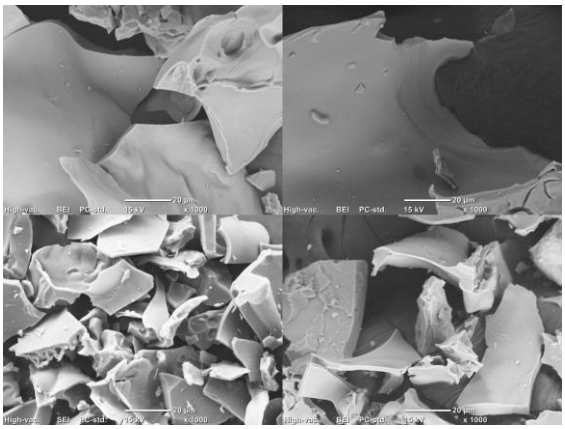

b

Fig. 1. a – SEM images of the Eu^{3+} doped Al_2O_3 samples at 1.5 % (top left), 3.0 % (top right), 5.0 % (bottom left) and 7.0 % (bottom right) for under 1000× magnification; b – XRD patterns of the Eu^{3+} doped Al_2O_3 samples

2.5. Photoluminescence spectra analysis

The emission spectra analysis of $Al_2O_3:xEu^{3+}$ fingerprint developer powder samples provides valuable insights into the luminescent properties at varying Eu^{3+} doping concentrations, as illustrated in Fig. 2 a. Notably, all luminescent powders exhibit emission peaks at 615 nm, 650 nm, and 700 nm, resulting in intense red emission under excitation with ultraviolet light at a wavelength of λ_{exc} = 254 nm. The most prominent peak, centered at λ = 615 nm, corresponds to the $^5D_0$-$^7F_2$ 4f-4f forbidden transition of Eu^{3+} [11]. Similarly, the peaks at 650 nm and 700 nm correspond to the forbidden transitions $^5D_0$-$^7F_3$ and $^5D_0$-$^7F_4$, respectively [12]. Conversely, the pure undoped sample shows no luminescent emission (though its spectrum

is included for comparison). At a low doping concentration of x = 1.5 % Eu, minimal emission is observed. Subsequently, with x = 3.0 % Eu doping, the most intense luminescent emission is achieved, as evident in Fig. 2 a. However, as the Al_2O_3 matrix is doped further with x = 5.0 % Eu, the luminescent emission diminishes, and with x = 7.0 % Eu doping, the intensity drops dramatically, even lower than that of the x = 1.5 % Eu-doped sample. This phenomenon is attributed to luminescent inhibition due to concentration effects, as reported by G. Blasse and B.C. Grabmaier [13].

The CIE coordinates for the emission of the Eu^{3+} doped Al_2O_3 phosphors in Fig. 2 b reveal a notable trend in the CIE 1931 color coordinates as the concentration of Eu^{3+} decreases. The coordinates shift from (x = 0.5347, y = 0.3153) at 0.07 mol to (x = 0.56783, y = 0.32922) at 0.015 mol, indicating a transition from a red-orange hue to lighter orange tones. This variation in color coordinates underscores the significant influence of Eu^{3+} on the optical properties of the Al_2O_3 matrix. The dopant modifies the electronic structure and energy levels, resulting in distinct emissions in the visible spectrum.

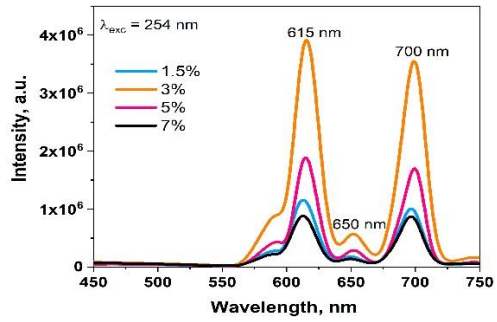

a

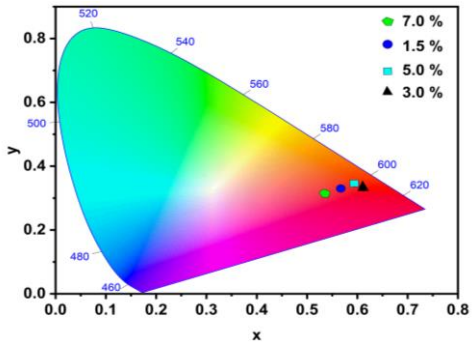

b

Fig. 2. a – PL spectra of the Eu^{+3} doped Al_2O_3 at the different concentrations excited at 254 nm; b – CIE coordinates for the emission of the Eu^{3+} doped Al_2O_3 phosphors (1.5, 3.0, 5.0 and 7.0 %)

3. RESULTS

The synthesis successfully produced the Al_2O_3 phase, as confirmed by X-ray diffraction analysis. Scanning Electron Microscopy (SEM) revealed that the material consists of the sheet with an average particle size of 177.88 µm. This level of uniformity makes the sheet particularly suitable for fingerprint detection applications that utilize phosphorescent powders. Such powders rely on larger particle sizes to enhance their luminescent properties, which improve visibility and adherence to fingerprint residues. This contrasts with non-phosphorescent materials, where smaller particle sizes are typically employed to optimize coverage and resolution in fingerprint development [14].

The crystalline phase obtained through the combustion method has one major added advantage: scalability of synthesis. This lays the ground for possibly commercializing phosphor. Besides, phosphorescent materials can be applied on any surface, including fluorescent ones, which generally hinder proper development and obscure key pattern identifications in fingerprints [7]. This, therefore, solves one major problem in forensic fingerprint detection. Furthermore, the innovative application of these materials in practical forensic scenarios, combined with their demonstrated efficacy on surfaces like steel, plastic, and ceramic, distinguishes this work from previously published studies.

Detecting fingerprints is crucial in criminal investigations, and luminescent materials play a pivotal role in this process [14]. These materials emit light when excited by an energy source, such as ultraviolet radiation. This allows for the revelation of latent fingerprints that are not visible to the naked eye [15]. The application of luminescent materials in fingerprint detection provides an effective tool for forensic investigators, enabling them to identify and analyze crucial evidence at the crime scene, even on challenging surfaces or under adverse lighting conditions [15].

The fingerprint samples were obtained from male volunteers who provided informed consent for the research, ensuring they were healthy individuals aged between 23 and 28 years, free from any cutaneous pathologies that could potentially affect the experimental outcomes. Before to sample collection, the donors washed their hands to eliminate any potential contamination, followed by the deposition of fingerprints on various objects, including a knife, cup, bank card, and prescription glasses, using scalp and/or facial oils as bait. Utilizing alumina synthesized with a 3.0 % europium concentration, selected for its superior luminescence, the powder was sprinkled onto the fingerprints. Excess powder was removed, and photographs were taken using a cell phone camera under both white light and ultraviolet (UV) illumination.

The ceramic cup in Fig. 3 a is composed of a mixture of clay, silica, feldspar, and a black glaze coating [16]. The fingerprint acquisition technique was applied to this surface and revealed under sunlight and UV lamp illumination, as observed at the top right and bottom right, respectively.

Fig. 3 b depicts a knife with the powders applied to the fingerprints, illuminated with visible light. Subsequently, photographs of the fingerprints under visible light and UV light were captured for analysis (bottom left and bottom right, respectively). The knife used corresponds to a martensitic stainless steel material from the 410 series of the American Iron & Steel Institute (AISI), featuring a composition of 0.15 % carbon, 1.00 % manganese, 1.00 % silicon, 11.5 – 13.5 % chromium, 0.004 % phosphorus, and 0.03% sulfur [17].

The bank card of Fig. 3 c is made of PVC, a polyvinyl chloride composite material [12], and fingerprints were revealed under visible and UV light (bottom left and bottom right).

Finally, Fig. 3 d shows spectacles. The material used to make the lenses is polycarbonate, which is composed of bisphenol-A (BPA), also fingerprints were revealed under the same conditions as the other surfaces (bottom left and bottom right).

3. DISCUSSION

The detection of fingerprints using alumina powders presents various challenges depending on the surface material. On mixtures of silica and clay, such as ceramic surfaces, the porous and uneven texture can make it difficult for the powder to adhere uniformly, complicating the visualization of clear fingerprint patterns [18]. Stainless steel, particularly martensitic types, often have a smooth and reflective surface that can cause the powder to slide off or create glare, hindering accurate fingerprint detection [19]. PVC, commonly used in items like bank cards, has a non-porous but flexible nature that might lead to incomplete or smudged prints when the powder is applied [20]. Finally, surfaces made of polycarbonate with bisphenol-A (BPA), like those of prescription glasses, are not only smooth and hard but also prone to static electricity, which can cause the powder to disperse unevenly and obscure the fine details of the fingerprints [21]. However, using phosphorescent alumina instead of regular alumina offers a significant advantage. The phosphorescent properties allow the powder to emit light under UV illumination, enhancing the contrast and visibility of latent fingerprints even on challenging surfaces [7]. This luminescent effect improves the detection and analysis of fingerprint patterns, making it a valuable tool in forensic investigations [7].

The analysis of the images obtained from Fig. 3 revealed the presence of distinctive characteristics typical of fingerprints. These images clearly show the unique patterns of arches, loops, and whorls, which are consistent with the features found in human fingerprints. Furthermore, it was observed that these fingerprints exhibit notable durability, suggesting that the identifying patterns remain unchanged over time. These findings confirm the efficacy of the fluorescent material Al_2O_3:xEu^{3+} in the revelation and visualization of fingerprints, highlighting its utility in forensic and security applications. The europium-doped alumina powder proved to be highly effective in fingerprint detection on a variety of surfaces, including metals (AISI 410 steel), ceramics (clay), and polymers (PVC and BPA).

a

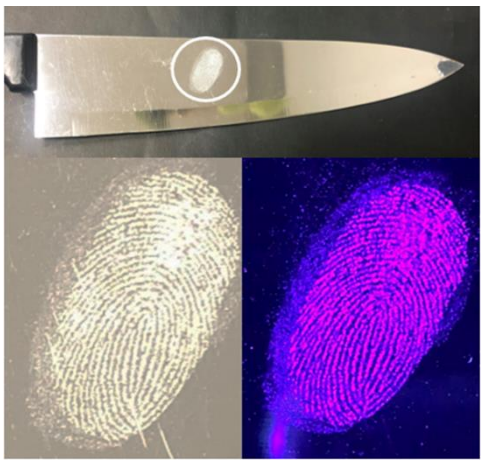

b

c

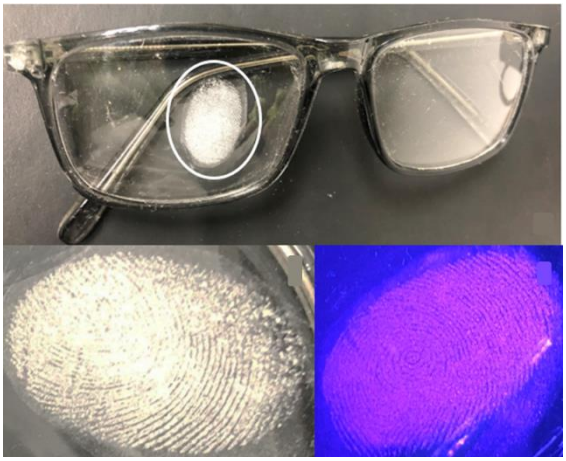

d

Fig. 3. Fingerprint development a – on a knife, illuminated with visible light and (top right) under UV light. (bottom right) on a cup; b – illuminated with visible light (bottom left) and under UV light (bottom right); c – on a bank card, illuminated with visible light (bottom left) and under UV light (bottom right); d – on graduation lenses, illuminated with visible light (bottom left) and under UV light (bottom right)

The application of this powder on the mentioned surfaces allowed for successful fingerprint collection, providing a versatile and reliable method for forensic investigation.

4. CONCLUSIONS

Based on the findings presented in this study, Al_2O_3:xEu^{3+} red phosphors synthesized through combustion synthesis exhibited promising properties for application in forensic fingerprint detection. The X-ray diffraction analysis confirmed the crystalline phase of the produced powders, while scanning electron microscopy revealed a sheet-like morphology with particle sizes ranging from 40 to 280 µm and an average thickness of 4.8 µm. Photoluminescence measurements under 254 nm excitation revealed two main red emission peaks attributed to Eu^{3+} luminescent transitions. Subsequent application of the Al_2O_3:xEu^{3+} red phosphors for fingerprint detection on various surfaces commonly found at crime scenes, including steel, plastic, and ceramic, resulted in the successful revelation of fingerprints. The photographs captured clearly depicted fingerprint features such as short ridges, eyes, bifurcations, cores, and right loop elements with sharpness and clarity. These results highlight the potential of Al_2O_3:xEu^{3+} red phosphors as an effective powder for fingerprint detection in forensic science applications, offering a valuable tool for criminal investigations.

Acknowledgments

The authors express their sincere gratitude to the National Council of Humanities, Science, and Technology (CONAHCYT) for their invaluable financial and logistical support. The authors acknowledge Dr. Alejandro Santibañez and Dr. Ernesto Hernandez from Centro de Investigación en Quimica Aplicada LANIAUTO for the XRD and SEM characterizations support.

REFERENCES

1. **Tian, X., Lian, S., Wen, J., Ji, C., Chen, Z., Peng, H., Li, J., Wang, S., Hu, J., Zhu, L., Peng, Y.** Microwave/starch-assisted Sol-Gel Synthesis and Photoluminescence of Eu^{3+}-doped α-Al_2O_3 Micro/Nano-Biscuits *Journal of Luminescence* 207 2019: pp. 301 – 309. https://doi.org/10.1016/j.jlumin.2018.10.068
2. **Das, A., Shama, V.** Synthesis and Characterization of Eu^{3+} Doped α-Al_2O_3 Nanocrystalline Powder for Novel Application in Latent Fingerprint Development *Advanced Materials Letters* 7 2016: pp. 302 – 306. https://doi.org/10.5185/amlett.2016.6310
3. **Choudhury, I.A., Kafy, A., Rahman, A., Pranto, M.T.A.** Review of Recent Developments in Processing and Application of Aluminum Matrix Composites with Alumina Particles *Comprehensive Materials Processing (Second edition)* 12 2024: pp. 429 – 441. https://doi.org/10.1016/B978-0-323-96020-5.00053-4
4. **Kim, D., Kim, H.E., Kim, C.H.** Enhancement of Long-Persistent Phosphorescence by Solid-State Reaction and Mixing of Spectrally Different Phosphors *ACS Omega* 5 2020: pp. 10909 – 10918. https://doi.org/10.1021/acsomega.0c00620
5. **Baudín, C.** Alumina, Structure and Properties *Encyclopedia of Materials: Technical Ceramics and Glasses* 2021: pp. 25 – 46. https://doi.org/10.1016/B978-0-12-818542-1.00028-X
6. **Liu, D., Zhu, Z.** Photoluminescence Properties of the Eu-doped alpha-Al_2O_3 Microspheres *Journal of Alloys and Compounds* 583 2014: pp. 291 – 294. https://doi.org/10.1016/j.jallcom.2013.08.173
7. **Chávez, D., Garcia, C.R., Oliva, J., Diaz-Torres, L.A.** A Review of Phosphorescent and Fluorescent Phosphors for Fingerprint Detection *Ceramics International* 47 2021: pp. 10 – 41. https://doi.org/10.1016/j.ceramint.2020.08.259
8. **Patil, K.C., Hedge, M.** Nanocrystalline Oxide Materials, 1st ed. World Scientific Publishing, Singapore, 2008.
9. **Feret, F.R., Roy, D., Boulanger, C.** Determination of Alpha and Beta Alumina in Ceramic Alumina by X-ray Diffraction *Spectrochimica Acta B: Atomic Spectroscopy* 55 2000: pp. 1051 –1061. https://doi.org/10.1016/S0584-8547(00)00225-1
10. **Das, A., Shama, V.** Synthesis and Characterization of Eu^{3+} Doped α-Al_2O_3 Nanocrystalline Powder for Novel Application in Latent Fingerprint Development *Advanced Materials Letters* 7 2016: 302 – 306. https://doi.org/10.5185/amlett.2016.6310
11. **Bhagya, N.P., Prashanth, P.A., Krishna, R.H., Nagabhushana, B.M., Raveendra, R.S.** Photoluminescence Studies of Eu^{3+} Activated $SrTiO_3$ Nanophosphor Prepared by Solution Combustion Approach *Optik (Stuttgart)* 145 2017: pp. 678 – 687. https://doi.org/10.1016/j.ijleo.2017.07.003
12. **Llobet, E.** Gas Sensors using Carbon Nanomaterials: A Review *Sensors and Actuators B: Chemical* 179 2013: pp. 32 – 45. https://doi.org/10.1016/j.snb.2012.11.014
13. **Blasse, G., Grabmaier, B.C.** Luminescent Materials. Springer Berlin Heidelberg, Berlin, Heidelberg. 1994: pp. 165 – 190. https://doi.org/10.1007/978-3-642-79017-1
14. **Huynh, C., Halámek, J.** Trends in Fingerprint Analysis *TrAC – Trends in Analytical Chemistry* 82 2016: pp. 328 – 336. https://doi.org/10.1016/j.trac.2016.06.003
15. **Tapps, M., McMullen, L., Gagné, M.E., Beaudoin, A.** Revealing a Decades-old Fingermark with Cyanoacrylate Fuming and Rhodamine 6G *Forensic Science International* 300 2019: pp. e9 – e12. https://doi.org/10.1016/j.forsciint.2019.04.025
16. **Cely-Illera, L., Bolívar-León, R.** Materia Prima para la Industria Cerámica de Norte de Santander. II. Evaluación del Comportamiento Térmico y su Incidencia en las Propiedades Tecnológicas *Respuestas* 20 2015: pp. 84 – 94. https://doi.org/10.22463/0122820X.260
17. **Garrison, W.M., Amuda, M.O.H.** Stainless Steels: Martensitic *Reference Module in Materials Science and Materials Engineering* 2017: pp. 120 – 156. https://doi.org/10.1016/B978-0-12-803581-8.02527-3
18. **Deans, J.** Recovery of Fingerprints from Fire Scenes and Associated Evidence *Science & Justice* 46 2006: pp. 153 – 168. https://doi.org/10.1016/S1355-0306(06)71589-1
19. **Barros, H.L., Stefani, V.** Micro-structured Fluorescent Powders for Detecting Latent Fingerprints on Different Types

of Surfaces *Journal of Photochemistry and Photobiology A: Chemistry* 368 2019: pp. 137 – 146. https://doi.org/a10.1016/j.jphotochem.2018.09.046

20. **Chavez, D., Garcia, C.R., Ruiz-Martinez, I., Oliva, J., Rivera-Rosales, E., Diaz-Torres, L.A.** Fingerprint Detection on Low Contrast Surfaces Using Phosphorescent Nanomaterials *AIP Conference Proceedings* 2083 2019: pp. 304 – 316. https://doi.org/10.1063/1.5094304

21. **Zhang, J., Zhang, X., Dediu, L., Victor, C.** Review of the Current Application of Fingerprinting Allowing Detection of Food Adulteration and Fraud in China *Food Control* 22 2011: pp. 1126 – 1135. https://doi.org/10.1016/j.foodcont.2011.01.019